Visual Comput (2007) 23: 743–751
DOI 10.1007/s00371-007-0156-1

ORIGINAL ARTICLE

Matthias Specht
Renaud Lebrun
Christoph P.E. Zollikofer

Visualizing shape transformation between chimpanzee and human braincases

Published online: 9 June 2007

M. Specht (✉) · R. Lebrun · C.P.E. Zollikofer
Anthropological Institute,
University of Zürich,
Winterthurerstr. 190, 8057 Zürich,
Switzerland
specht@corebounce.org,
renaud_lebrun@yahoo.fr,
zolli@aim.unizh.ch

Abstract The quantitative comparison of the form of the braincase is a central issue in paleoanthropology (i.e., the study of human evolution based on fossil evidence). The major difficulty is that there are only few locations defining biological correspondence between individual braincases. In this paper, we use mesh parameterization techniques to tackle this problem. We propose a method to conformally parameterize the genus-0 surface of the braincase on the sphere and to calibrate the parameterization to match biological constraints. The resulting consistent parameterization gives detailed information about shape differences between the braincase of human and chimp. This opens up new perspectives for the quantitative comparison of "featureless" biological structures.

Keywords Scientific visualization · Surface parameterization · Morphing · Brain · Geometric morphometrics

1 Introduction

Two major features discriminate our own species (*Homo sapiens*) from our closest living relatives, the chimpanzees (*Pan troglodytes*): we walk on two legs and have comparatively big brains. It is still a matter of debate how and why during human evolution brain size was increased, and what makes the principal difference between a human and a chimpanzee brain, or between the braincase of a fossil and a modern human. One important prerequisite to tackle these questions is to quantify the form of the bony case containing the brain (the brain *endocast*, see Fig. 1), because the braincase is the only comparative data source in fossil humans and in ape specimens housed in collections worldwide.

Quantitative comparison of biological form is a notoriously difficult task. This is because the geometry of biological forms is typically more complex than that of standard Euclidean bodies and graphic primitives, such that classical ruler-based measurements, e.g., linear distances between reference points, only capture a small fraction of potentially relevant morphological information. Free-form object representation by surface triangulation into a triangle mesh is an important first step to quantify biomedical objects. However, once we have reconstructed a series of free-form surfaces of braincases, how can we perform quantitative comparative analyses of their shape?

Any biologically sensible comparison relies on the definition of so-called homology relationships. Homology denotes biological equivalence through evolutionary and developmental history. For example, the brain of individual A is homologous to the brain of individual B, and a point on the tip of the nose of individual A is homologous to the tip of the nose of individual B. The tip of the nose is an example for a *point homology* or *landmark*.

Interestingly, close analogies exist between the definition of homology between biological structures and the concept of surface parameterization in computer graphics. In both instances, morphing of shape A into shape B relies on a set of matching feature points that define a transformation function. The traditional tool of *geometric morphometrics* to define such a transformation is the thin-plate spline (TPS) [5]. The spline function quantifies the biologically relevant difference between the two shapes and can be used to measure and visualize local versus global shape

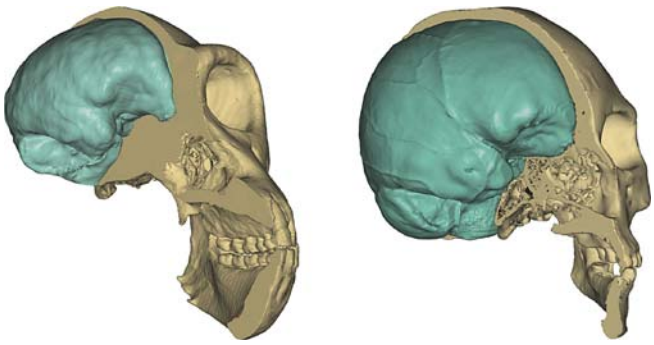

Fig. 1. Brain endocasts (*light green*) of a chimp (*left*) and a modern human (*right*)

differences. For example, while the face (or facial skeleton) of humans and apes is rich in well-defined anatomical landmarks (such as the tip of the nose, the center of the eye, etc.), the braincase (and even the brain) is not. On the face, landmarks are typically defined at meeting points between three or more adjacent structures, or at extremal locations. Because of the lack of landmarks, splines are difficult to apply to the braincase.

In computer graphics, methods of *consistent mesh parameterization* deal with a similar problem, the simultaneous parameterization of several surfaces on a common parameter domain such that a given set of user-specified features match.

In this paper, we examine how concepts of mesh parameterization can be combined with concepts of geometric morphometrics to obtain consistent quantitative descriptions of relatively "featureless" genus-0 structures such as the braincase. First we conformally map the surfaces to the sphere. Then we deform the spherical parameterizations such that the biological features match. The resulting well-defined consistent parameterization captures the geometry and matches biological constraints. Finally, we apply these methods to compare the shape of the braincases of chimpanzees and humans and we show how to visualize the differences.

2 Related work

In order to compare shapes given in the form of triangle meshes, we need (1) a method to establish point-to-point correspondence on the surfaces and (2) methods to visualize shape difference (or the transformation from one shape into another). In this section we look at previous work in these areas.

2.1 Establishing point-to-point correspondence on a set of surfaces

Semilandmarks. One approach to tackle the problem of missing landmarks is to fill landmark-depleted regions of the surfaces with additional points of reference, so-called semilandmarks [6]. They are usually applied on 2D outlines. Extensions to 3D exist [2, 15], but typically, these techniques are based on ad hoc template definitions, and not used for visualization purposes.

Surface parameterization and distortion metrics. Parameterization of triangle meshes in 3D on a simpler domain such as a planar region, the sphere or a simplicial domain is a key problem for many applications in computer graphics and has received much attention. We refer to the comprehensive surface parameterization survey in [8]. There are always two problems to solve: (1) no foldovers and (2) minimization of a distortion metric. In general, it is not possible to find an *isometric* mapping, i.e., a mapping which preserves distances or both angles and area. Therefore, depending on the application, either area or angle distortion or a combination of them is minimized, and many methods have been proposed. Of special interest are *conformal* mappings which preserve the angles of the triangulation. Conformal mappings have a connection to complex function theory, locally preserve geometry and have less degrees of freedom than mappings which preserve area. Equi-areal mappings, on the other hand, are interesting because they assign the same amount of parameter space to every surface element (uniformity). In practice, often some functional which is a combination of angle distortion and area distortion is minimized to balance between the two extremes.

Examples are the stretch metric [23] and the harmonic map [7]. Maps with minimal stretch are often called "quasi-isometric" and tend to uniformly distribute samples on the surface when the parameter domain is uniformly sampled. Harmonic maps are a superset of conformal maps and therefore not angle preserving in general; however, they minimize deformation in the sense that they minimize the Dirichlet energy. Harmonic maps are well-studied for the planar case and are relatively easy to compute.

Spherical parameterization. Parameterizing an arbitrary genus-0 surface on the sphere has received much attention in recent years (see for instance [1, 10, 14, 16, 20, 22]). Our work is based on the *global conformal parameterization* introduced by Gu and Yau [13, 14]. The parameterization is called global because it preserves the conformality everywhere. They exploit the fact that on the sphere, a harmonic map is also a conformal map. All conformal maps to the sphere form a Moebius group with only six degrees of freedom (three of those are the rotations around the coordinate axes). Gu and Yau define a unique solution by adding an additional constraint and also point out that the conformal map is solely defined by the geometry and not by the triangulation because it preserves the shape locally. These two properties (well-defined solution and preservation of geometry) are important prerequisites for our application.

Consistent parameterization. In the pioneering work [21], a set of genus-0 surfaces was consistently parameterized with respect to a (user-specified) base domain. The parameterizations are *consistent* because they give immediate correspondences between models and allow remeshes with the same connectivity.

Later work [19, 24] presented techniques which do not require the connectivity of the base domain to be defined by the user and are able to handle models of higher genus. However, these methods are limited to two or three surfaces to be parameterized because they avoid a simple common parameter domain.

Asirvatham et al. [3] proposed to use the sphere as a common parameter domain. They employ a variant of the spherical parameterization algorithm from [20] to map a set of genus-0 surfaces to the sphere such that manually labeled features match. The surface in-between the feature points, however, is parameterized using random searches to minimize the stretch metric until a local minimum is found. This gives visually satisfactory results but is not adequate for comparative analysis.

Brain mapping. This is an example of a relevant application of the methods described above. Many approaches exist to map cortical surfaces of different individuals into a canonical space where they can be compared numerically or visually. This is a scenario similar to ours, and conformal mappings received much attention [12]. It is often desirable that landmarks are mapped onto each other in parameter space and landmark matching has been studied intensively. The work in [26] and [28] introduce additional constraints to the algorithm for the conformal mapping.

However, we are not only interested in aligning the surfaces in both real and parameter space, but we want to measure (and visualize) the actual deformation between the surfaces. We use the method proposed by Glaunès et al. [9] to calculate large deformation diffeomorphisms of the sphere onto itself, given a source and a target set of landmarks.

2.2 Visualization of shape transformation

A traditional way to visualize shape deformation in 2D are *deformation grids*. An image is overlaid with a Cartesian coordinate system and the TPS is calculated, which deforms the image such that the homologies match a target configuration. Applying the spline on the coordinate system results in a deformed grid. Thompson [25] introduced hand-drawn deformation grids to visualize shape transformation of related biological forms. Bookstein [5] formalized the approach. Previous attempts to directly extend the deformation grids from 2D to 3D (by either 3D cuboid grids or 2D square grids positioned in space) were problematic from a biological point of view [27].

Alternatively, once point-to-point correspondence is determined on two or more surfaces, the difference can be calculated in the form of scalar or vector fields, statistically analyzed and visualized on the actual surface using standard scientific visualization methods like false-color mapping or annotation with glyphs (icons) [27].

2.3 Contribution

First, we are going to propose a method to consistently parameterize a set of genus-0 surfaces on the sphere. Every vertex of the original meshes is mapped to a well-defined position on the sphere. Second, we are going to exploit the quasi-conformality of the parameterization to draw an orthogonal (θ, ϕ) coordinate system on the surface. This resembles the 2D deformation grids and forms a new approach to use the concept on 3D surfaces.

3 Consistent quasi-conformal map to the sphere

In this section we present our main contribution, the method to calculate a well-defined consistent parameterization for a set of genus-0 surfaces. Figure 2 gives a pictorial explanation of the procedure.

We have a set of N_S endocranial surfaces M_i, represented as triangle meshes. On every surface, a set L_i of N_L points $\boldsymbol{l}_{i,j}$ is manually labeled. The sets L_i indicate biological correspondence across the surfaces.

Our goal is to find a unique bijective mapping $\boldsymbol{h}_i$ from each surface M_i to the sphere S^2

$$\boldsymbol{h}_i : M_i \to S^2 : (x, y, z) \mapsto (\theta, \phi), \quad i \in [1, N_L]\,. \tag{1}$$

The requirements are:

1. For all surfaces, points of biological homology map to the same positions $\boldsymbol{p}_j$ in parameter space, i.e.,
$$\boldsymbol{h}_1(\boldsymbol{l}_{1,j}) = \boldsymbol{h}_2(\boldsymbol{l}_{2,j}) = \ldots = \boldsymbol{h}_{N_S}(\boldsymbol{l}_{N_S,j}) = \boldsymbol{p}_j\,. \tag{2}$$
2. The surface between the landmarks is mapped such that geometrical features match as well as possible under the biological constraints.

In order to find a unique solution, we use the fact that a conformal map from a surface to the sphere has only six degrees of freedom, three of which are rotations. This is because a conformal map can be composed with any conformal map from the sphere onto itself to form a new conformal map. So, additional constraints are needed. Haker et al. [16] fix three points on the sphere and Gu and Yau [13] propose the zero-mass center constraint:

$$\int_{M_i} \boldsymbol{f}\, d\sigma_{M_i} = 0 \tag{3}$$

where $d\sigma_{M_i}$ the area element on M_i. Equation 3 defines a solution $\boldsymbol{f}$, which is unique up to the three rotations. We use their algorithm to compute a unique spherical confor-

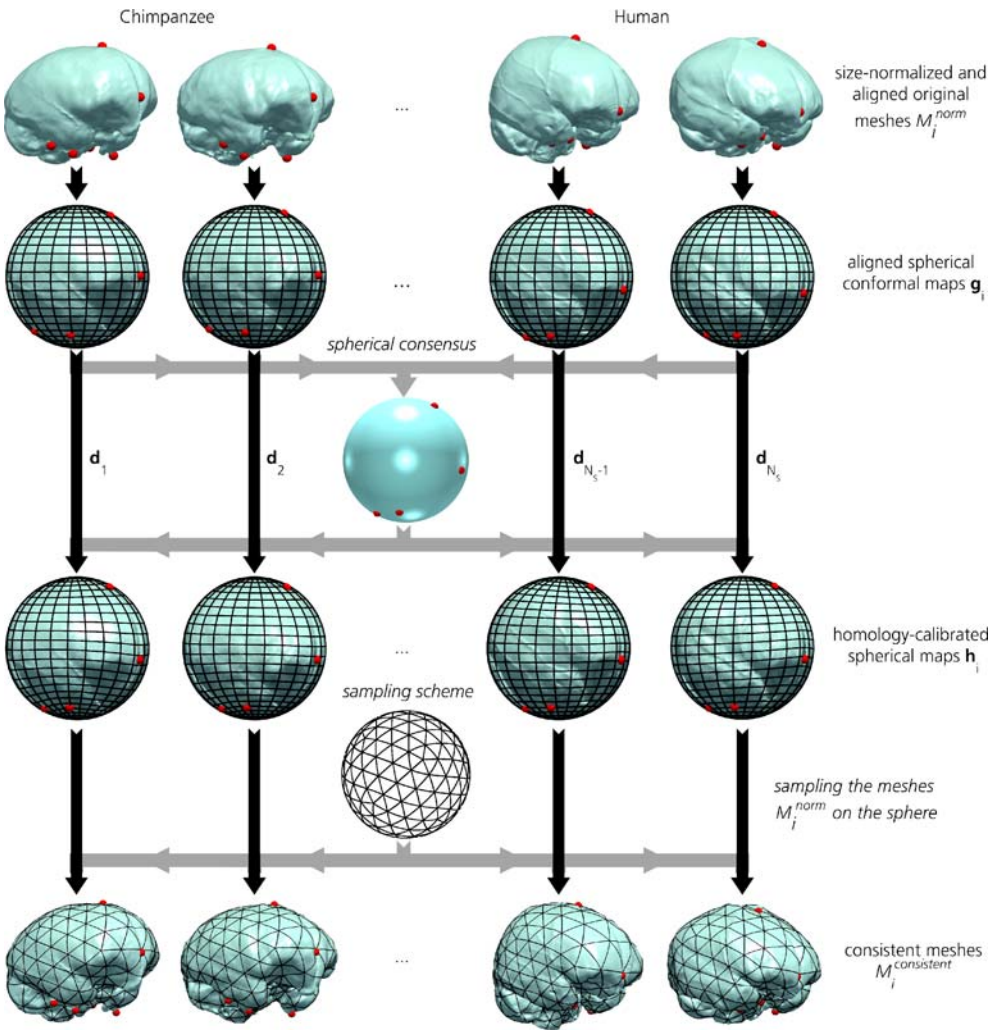

Fig. 2. Pictorial overview of the calculation of our consistent quasi-conformal spherical parameterization. The original surfaces are conformally mapped to the sphere; there maps are deformed such that the biological features (homologies) match their spherical consensus. The spherical domain is then sampled with a Loop-subdivided spherical icosahedron to consistently remesh the original surfaces

mal map $\boldsymbol{f}_i$ for each surface M_i. Conformal maps locally preserve geometry, so the $\boldsymbol{f}_i$ fulfill the second requirement from above.

Area and distances are distorted however. More precisely, they are changed by a scaling factor (the so-called conformal factor) depending on the position on the surface. It is desirable to have a uniform (i.e., equi-areal) parameterization because uniform sampling is important for discrete function approximation and analysis. As mentioned, it is not possible to avoid both angle and area distortion. A way to find the most uniform conformal parameterization has been proposed in [17]. However, the nature of our data (no extreme extrusions) and the zero-mass center condition prevent extreme area distortion.

In order to fulfill the first requirement, we need to find good positions for the images of the landmarks on the sphere and then deform the conformal maps such that the images of the landmarks match on the sphere.

We rigidly align the spherical parameterizations $\boldsymbol{f}_i$ by generalized least squares minimization (GLS) of the spherical landmark distances to obtain the aligned sets $\boldsymbol{g}_i$. We use an algorithm based on the one from Gower [11] but adapted to spherical geometry (i.e., no translation step and projection of the mutual mean to the sphere). The *spherical consensus* C is the set of mean landmarks $\boldsymbol{c}_j$ on the sphere:

$$\boldsymbol{c}_j = normalize\Big(\sum_{i=1}^{N_S} \boldsymbol{g}_i(\boldsymbol{l}_{i,j})\Big), \quad j \in [1, N_L]\,. \tag{4}$$

The aligned maps $\boldsymbol{g}_i$ must now be deformed such that the associated landmark sets L_i match C. We use the algorithm from [9] to construct a deformation map $\boldsymbol{d}_i : S^2 \mapsto S^2$ such that:

$$\boldsymbol{d}_i(\boldsymbol{g}_i(\boldsymbol{l}_{i,j})) = \boldsymbol{c}_j \quad \forall \text{ points } \boldsymbol{l}_{i,j} \tag{5}$$

for each surface by integration of velocity fields that minimize a quadratic smoothness energy under the landmark constraint $L_i \to C$ on the sphere.

The conformal maps $\boldsymbol{g}_i$ can be deformed with the deformation diffeomorphisms $\boldsymbol{d}_i$:

$$\boldsymbol{h}_i = \boldsymbol{d}_i \circ \boldsymbol{g}_i, \tag{6}$$

thus constraining the geometry with the biological data. Because both $\boldsymbol{d}_i$ and $\boldsymbol{g}_i$ are bijective, $\boldsymbol{h}_i$ is bijective as well, and so is $\boldsymbol{h}_i^{-1}$.

Since the smoothness energy minimized in Eq. 5 is based on geodesic distances, the deformations do not preserve angles, i.e., the $\boldsymbol{h}_i$ are not conformal anymore. We use this angle deformation to visualize shape transformation in the next section and call the maps quasi-conformal.

An important property of the deformation is uniqueness, inferring that the $\boldsymbol{h}_i$ are unique as well.

4 Visualizing shape difference

The mappings $\boldsymbol{h}_i$ are bijective and permit sampling the surfaces M_i over the spherical domain (using barycentric coordinates). However, to measure the difference in shape, it is important to remove differences in size, position and orientation between the objects. We size-normalize the original surface M_i by scaling all vertices such that the volume becomes equal to one:

$$M_i^{\text{norm}} = \frac{M_i}{\sqrt[3]{\text{volume}(M_i)}} \tag{7}$$

and minimize landmark variability by minimizing the sum of squared distances [11].

Sampling the surfaces over the spherical domain (i.e., the inverse mapping $\boldsymbol{h}_i^{-1}$) maps a sampling position (θ_k, ϕ_k) to a position $\boldsymbol{p}_k$ in R^3 onto the surface M_i^{norm} and results in a consistent remesh with the connectivity of the sampling scheme (see Fig. 2). The $\boldsymbol{p}_k^i$ are corresponding points and can directly be used for statistical analysis. For instance, the difference of two surfaces M_1 and M_2 is just the difference of all $\boldsymbol{p}_k^1$ and $\boldsymbol{p}_k^2$.

4.1 Drawing a consistent coordinate system on surfaces and texturing

Once a consistent parameterization for a set of surfaces is obtained, a coordinate system can be drawn on the parameterization domain and mapped to the surfaces. Corresponding points on each surface have the same spherical coordinates (θ, ϕ). Drawing an equi-angular coordinate system on the sphere produces spherical quadrangles with spherical angles approaching right angles ("orthogonal coordinate system"). A conformal map to a surface preserves the angles and produces approximations to rectangles on the surface. The stronger the (biologically defined) deformation $\boldsymbol{d}_i$ (Eq. 5), the larger the deviation from conformality; this is observable in the non-orthogonality of the grid on the surface, which resembles the mentioned deformation grids.

Spherical coordinates can be drawn on the surfaces as a wire frame on top of the surface. Using texturing as a more general approach, any rectangular image can be used to texture the surface since the spherical coordinates can directly be used as texture coordinates:

$$u = \frac{\phi}{2\pi}, \quad v = \frac{\theta}{\pi}\,. \tag{8}$$

The positions of the M_i^{norm} and the spherical coordinate system are important for the visual appearance of the deformation grid. If a subset of the landmarks defines a symmetry plane, we can use them to position the M_i^{norm} in a canonical way: we rotate all surfaces such that the symmetry plane of the average surface lies in the xz-plane.

We usually position the coordinate system such that the poles are on the y-axis and the 0-meridian passes through $(0, 0, 1)$.

However, the poles of the spherical coordinate system are problematic areas for visualization. When there is no need for a specific position of the coordinate system in space, we can fix the spherical grid to the camera such that the poles are always on top and bottom. In practice, if we look at a surface in a 3D viewer and rotate the object relative to the camera with rotation matrix A, we transform the texture coordinates with A^T. This resembles the projective texture mapping technique where a (planar) image is projected onto a 3D scene, like a slide projection.

4.2 Morphing

Our parameterization permits the definition of a morphing function from the surface M_{from} to surface M_{to} by linear vertex interpolation:

$$\boldsymbol{p}_{\text{inter}}^k(t) = (1-t)\cdot \boldsymbol{p}_{\text{from}}^k + t \cdot \boldsymbol{p}_{\text{to}}^k, \quad t \in [0, 1]\,. \tag{9}$$

Combined with displaying an orthogonal coordinate system on the surface, interactive blending between the shapes is a very powerful way to explore shape difference.

4.3 Visualization of relative shape transformation on the surface

From the consistent parameterizations, scalar or vector fields can be calculated and visualized directly on the surface. We implemented the method for visualizing shape variation proposed in [27].

Direction and magnitude of shape transformation. To compare a surface M_i^{norm} to a reference surface M_R^{norm}, we calculate the displacement vector $\boldsymbol{d}^k$ for every spherical sampling position (θ_k, ϕ_k):

$$\boldsymbol{d}^k = \boldsymbol{p}_i^k - \boldsymbol{p}_R^k\,. \tag{10}$$

The displacement vector $\boldsymbol{d}^k$ is then decomposed into its normal and tangential components (relative to the surface in $\boldsymbol{p}_R^k$):

$$\boldsymbol{d}^k = \boldsymbol{d}_\perp^k + \boldsymbol{d}_\parallel^k, \tag{11}$$

where $\boldsymbol{d}_\parallel^k$ is visualized as an arrow glyph attached to $\boldsymbol{p}_i^k$, and the length and direction of $\boldsymbol{d}_\perp^k$ is color-coded on the surface.

Local growth. Local relative growth at vertex $\boldsymbol{p}^k$ on the surface can be calculated by comparing triangle areas:

$$b^k = \log\left(\frac{A_i^k}{A_R^k}\right), \tag{12}$$

with A_i^k the area of the 1-ring of $\boldsymbol{p}^k$ on M_i^{norm} and A_R^k the corresponding area on M_R^{norm}. The scalars b^k are visualized by coloring the surface.

5 Application and results

We implemented the methods proposed in this paper as parts of our MorphoTools Framework. MorphoTools is an application for 3D geometric morphometric analysis and visualization of the results. It permits interactive biological hypothesis refinement. The mesh processing methods from Sect. 3 are implemented in C++, using the OpenMesh[1] library. Visualization of the results, using the techniques described in Sect. 4, is implemented in Java with the aid of the Visualization Toolkit (VTK).[2]

We calculated homology-calibrated parameterizations for a test set consisting of endocranial surfaces of $N = 4$ humans and $N = 4$ chimpanzees.

Triangle meshes were manually segmented from volumetric CT scans using the software Amira.[3]. The endocranial surface of each individual was manually annotated with ($K = 7$) homologous landmarks (see Fig. 3), located at clearly recognizable foramina in the cranial base, and on well-defined points along the midplane of the braincase.

We used the tool ReMESH [4] to remove topological noise (i.e., make sure the meshes are genus-0) and to simplify the surfaces to 50 000 vertices prior to our parameterization.

As a sampling scheme we used an icosahedron projected to the sphere and subdivided seven times (Loop scheme), resulting in 163 842 consistent vertices which we call "semilandmarks". Each subdivision level contains the vertices of the previous level. This permits straightforward level-of-detail control by choosing the subdivision level for the reconstruction (we used this feature for drawing level-3 wire frames on top of level-7 meshes at the bottom of Fig. 2).

Since all vertices are consistent, principal component analysis (PCA) [18] can be used to measure the shape variance in the sample set. The first principal component, which comprises 82.13% of the total shape variation, distinguishes humans from chimpanzee endocasts (see Fig. 4). In the following, we visualize the transformation from the mean chimp to the mean human.

Figure 5 shows the morphing (Eq. 9) of a chimp into a human endocast and compares the performance of our new method with classical TPS-based morphing. The figure clearly shows the advantage of our method for such landmark-depleted forms: the thin-plate spline, defined purely by the landmarks, deforms the mean chimp surface such that the landmarks match the ones of the mean human. Since no landmarks are defined on the lateral parts, the TPS grossly misses the target surface in these areas. Clear differences can also be observed in the upper part of the back and the "nose" at the front.

Our method, in contrast, defines corresponding points everywhere on the actual surfaces, which results in a much more natural shape transformation.

Nr.	Description
1	frontalmost point on cortical surface
2	endobregma
3	sinus sigmoideus at deepest point
4,5	porus acusticus internus
6,7	foramen ovale

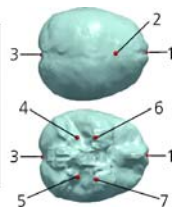

Fig. 3. The landmarks used for our analysis

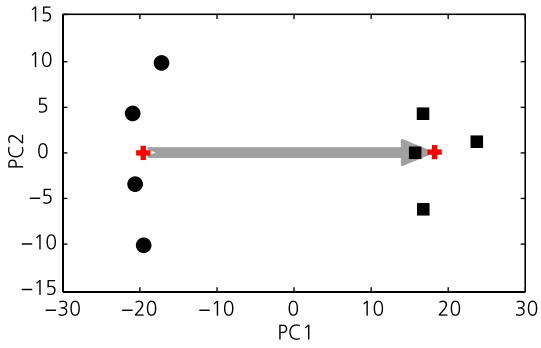

Fig. 4. Principal component analysis of the consistent remesh (163 842 "semilandmarks"). *Squares* represent humans; *circles* represent chimps. The *red crosses* and the *arrow* indicate the shape transformation along PC1 from the mean chimp to the mean human. PC1 comprises 82.13% of the total shape variation

[1] See http://www.openmesh.org for more information.
[2] See http://www.vtk.org for more information.
[3] See http://www.amiravis.com for more information

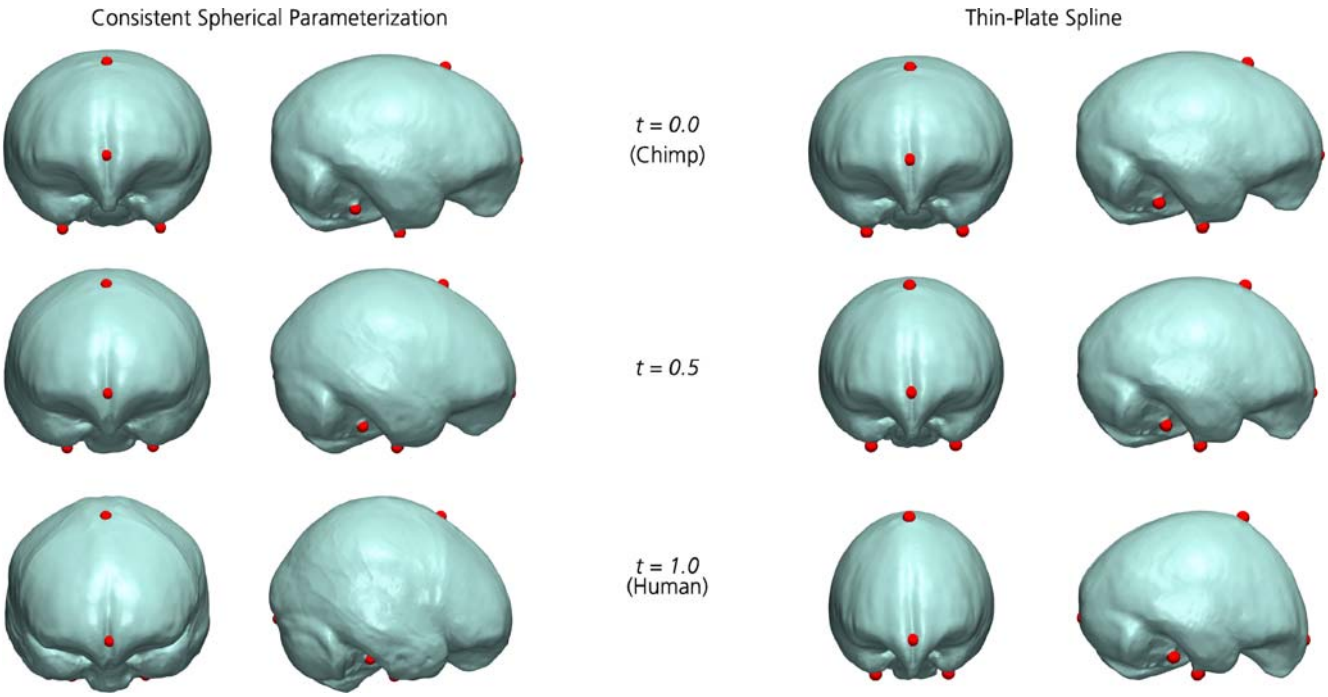

Fig. 5. Morphing from the mean chimp (*top row*) to the mean human (*bottom row*). Consistent Spherical parameterization (*left*), which defines corresponding points everywhere on the surfaces, is compared to thin-plate splines (*right*) which are defined by the seven landmarks only

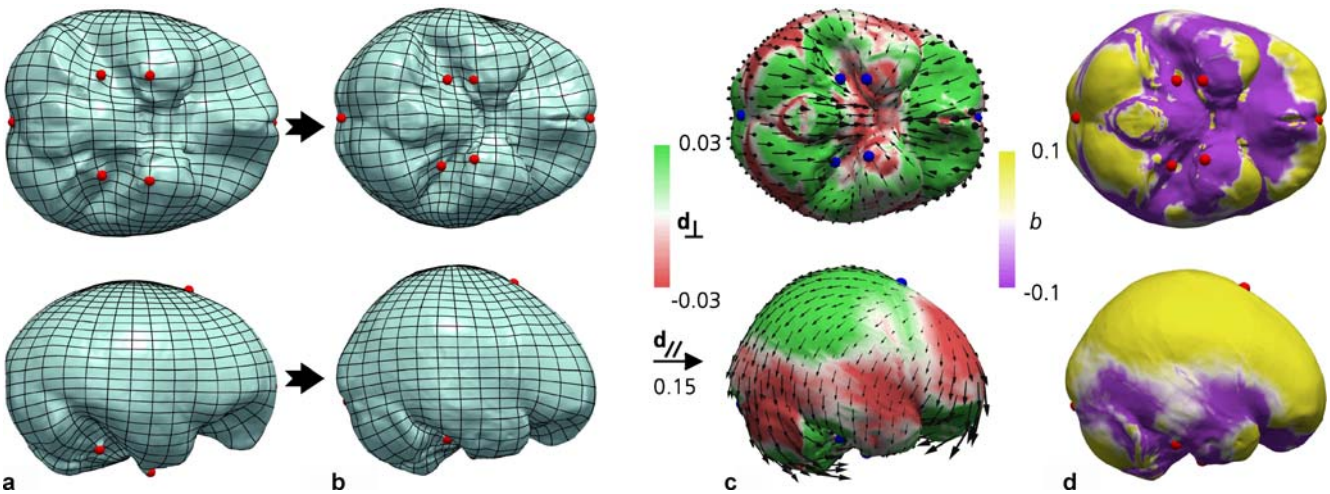

Fig. 6a–d. Visualizing shape transformation from chimp to human braincase. **a** The source surface (mean chimp braincase). **b** The target surface (mean human braincase) (both are overlaid with consistent spherical coordinate grids). **c**, **d** False-color map representation of the same transformation as in **a**, **b**. Graphs show mean human braincase, *red*/*green* indicate the direction (inward/outward) and magnitude of shape transformation perpendicular to the surface; arrows indicate shape change parallel to the surface. *Yellow*/*purple* indicate relative area expansion/contraction that was necessary to attain human shape

In Fig. 6, the techniques described in the previous section are used to visualize the shape transformation from a chimp braincase to a human braincase.

The pictures show that the spherical conformal parameterization, constrained with biological information, is well-suited to measure and visualize shape transformation of biological surfaces. Only a few landmarks are used but the patterns revealed are relatively complex and are clearly driven by geometrical features in-between the landmarks (for instance the lateral parts).

6 Conclusion and outlook

We have presented a method to constrain conformal spherical parameterizations of genus-0 surfaces with biological information (landmarks). The result is a parameterization which is (1) consistent from a biological point of view because the known point homologies are fixed points in the (spherical) parameter domain, and (2) quasi-consistent from a geometrical point of view because the parameterization is based on a conformal map (which is geometry preserving). The method was applied to quantify the surfaces of the braincase of chimpanzees and humans, and multiple visualization paradigms were used to explore the shape difference.

The resulting visualizations are very encouraging for further studies of shape variation of the braincase within our own species, and between closely related species. Studying larger samples with this method will permit answering important biological questions, for instance whether intraspecific variability is smaller than interspecific variability. For the emerging field of paleoneurology, the parameterization method proposed in this paper represents the first fully quantitative approach to compare complete endocranial surfaces. This is essential for biological research regarding our own evolution since it enables biologists to assess the braincase quantitatively (and therefore exploratively).

A limitation is the restriction to data without extreme extrusions, because the area distortion in the conformal map might become unacceptable. In [17], topological modification was suggested for such cases.

Acknowledgement We would like to thank Dr. Joan Glaunès for providing the code for calculating the deformations on the sphere and Dr. Jody Weissmann and Dr. Stefan Müller, as well as the anonymous reviewers, for helping to improve the manuscript. This research was supported in part by Swiss NSF grants 205321-102024/1 and 205320-109303/1.

References

1. Alexa, M.: Merging polyhedral shapes with scattered features. Vis. Comput. **16**(1), 26–37 (2000)
2. Andresen P.R., Nielsen, M.: Non-rigid registration by geometry-constrained diffusion. Med. Image Anal. **5**, 81–88 (2001)
3. Asirvatham, A., Praun, E., Hoppe, H.: Consistent spherical parameterization. Comput. Sci. ICCS 2005, PT 2 **3515**, 265–272 (2005)
4. Attene, M.: Remesh: an interactive and user-friendly environment for remeshing surface triangulations. Tech. Rep. 06/2004, IMATI-GE/CNR (2004)
5. Bookstein, F.: Principal warps: thin-plate splines and the decomposition of deformations. IEEE Trans. Pattern Anal. Mach. Intell. **11**(6), 567–585 (1989)
6. Bookstein, F.: Landmark methods for forms without landmarks: morphometrics in group difference in outline shape. Med. Image Anal. **1**, 225–243 (1997)
7. Eck, M., DeRose, T., Duchamp, T., Hoppe, H., Lounsbery, M., Stuetzle, W.: Multiresolution analysis of arbitrary meshes. In: Proceedings of ACM SIGGRAPH '95, pp. 173–182 (1995)
8. Floater, M.S., Hormann, K.: Surface parameterization: a tutorial and survey. In: N.A. Dodgson, M.S. Floater, M.A. Sabin (eds.) Advances in Multiresolution for Geometric Modelling, Mathematics and Visualization, pp. 157–186. Springer (2005)
9. Glaunès, J., Vaillant, M., Miller, M.I.: Landmark matching via large deformation diffeomorphisms on the sphere. J. Math. Imaging Vis. **20**(1–2), 179–200 (2004)
10. Gotsman, C., Gu, X., Sheffer, A.: Fundamentals of spherical parameterization for 3D meshes. Proc. ACM SIGGRAPH'03 **22**(3), 358–363 (2003)
11. Gower, J.C.: Generalized procrustes analysis. Psychometrika **40**(1), 33–35 (1975)
12. Gu, X., Wang, Y., Chan, T.F., Thompson, P.M., Yau, S.T.: Genus zero surface conformal mappings and its application to brain surface mapping. IEEE Trans. Med. Imaging **23**(8), 949–958 (2004)
13. Gu, X., Yau, S.: Computing conformal structures of surfaces. Commun. Info. Syst. **2**, 121–146 (2002)
14. Gu, X., Yau, S.T.: Global conformal surface parameterization. In: SGP '03: Proceedings of the 2003 Eurographics/ACM SIGGRAPH Symposium on Geometry Processing, pp. 127–137 (2003)
15. Gunz, P., Mitteroecker, P., Bookstein, F.L.: Semilandmarks in three dimensions. In: D.E. Slice (ed.) Modern Morphometrics in Physical Anthropology, chap. 3, pp. 73–98. Kluwer/Plenum, Dordrecht (2005)
16. Haker, S., Angenent, S., Tannenbaum, A., Kikinis, R., Sapiro, G., Halle, M.: Conformal surface parameterization for texture mapping. IEEE Trans. Vis. Comput. Graph. **6**(2), 181–189 (2000)
17. Jin, M., Wang, Y., Yau, S.T., Gu, X.: Optimal global conformal surface parameterization. In: Proceedings of the Conference on Visualization'04, pp. 267–274 (2004)
18. Jolliffe, I.: Principal Component Analysis. Springer, Berlin Heidelberg New York (1986)
19. Kraevoy, V., Sheffer, A.: Cross-parameterization and compatible remeshing of 3D models. In: Proceedings of ACM SIGGRAPH '04, pp. 861–869 (2004)
20. Praun, E., Hoppe, H.: Spherical parametrization and remeshing. Proc. ACM SIGGRAPH '03 **22**(3), 340–349 (2003)
21. Praun, E., Sweldens, W., Schröder, P.: Consistent mesh parameterizations. In: Proceedings of ACM SIGGRAPH '01, pp. 179–184 (2001)
22. Saba, S., Yavneh, I., Gotsman, C., Sheffer, A.: Practical spherical embedding of manifold triangle meshes. In: Shape Modeling and Applications, 2005 International Conference, pp. 256–265 (2005)
23. Sander, P.V., Snyder, J., Gortler, S.J., Hoppe, H.: Texture mapping progressive meshes. In: Proceedings of ACM SIGGRAPH '01, pp. 409–416 (2001)
24. Schreiner, J., Asirvatham, A., Praun, E., Hoppe, H.: Inter-surface mapping. In: Proceedings of ACM SIGGRAPH '04, pp. 870–877 (2004)
25. Thompson, D.W.: On Growth and Form. Cambridge University Press, Cambridge, UK (1917)
26. Wang, Y., Lui, L.M., Chan, T.F., Thompson, P.M.: Optimization of brain conformal mapping with landmarks. In: MICCAI (2), pp. 675–683 (2005)
27. Zollikofer, C.P., Ponce de León, M.: Visualizing patterns of craniofacial shape variation in homo sapiens. Proc. R. Soc. Lond. B Biol. Sci. **269**(1493), 801–807 (2002)
28. Zou, G., Hua, J., Gu, X., Xianfeng Muzik, X.: An approach for intersubject analysis of 3D brain images based on conformal geometry. In: International Conference on Image Processing ICIP 2006 (2006)

MATTHIAS SPECHT is currently a PhD candidate at the Morpholab of the Anthropological Institute at the University of Zürich. He received his MSc in computer science from ETH Zürich in 2000. His research interests focus on biologically meaningful surface parameterization and include interactive tools for 3D geometric morphometrics and visualization. He is further involved in the Corebounce Association's Soundium project, where he is co-developer of the multimedia engine Decklight.

RENAUD LEBRUN studied paleontology at the university of Montpellier, where he received a Master's degree. He is currently a PhD student at the Universities of Montpellier, France and Zürich, Switzerland where he studies the evolution of primates. His main field focuses on the comparison of the morphology of extant and fossil primates using computed tomography scans. Thus, he develops interactive tools to explore patterns of shape variability among large samples of 3D data.

CHRISTOPH P.E. ZOLLIKOFER studied biology at the University of Zürich, Switzerland, where he received a PhD in neurobiology. He is currently Professor of Anthropology at the Anthropological Institute of the University of Zürich. His main research field is computer-assisted anthropology, encompassing the investigation of patterns of morphological variability and evolutionary diversification in fossil and extant primates, computational modeling of morphogenetic processes, and development of image-based analytical tools for anthropology.